Two Barium Binding Sites on a Maxi K^+ Channel from Human Vas Deferens Epithelial Cells

Y. Sohma,* A. Harris,‡ C. J. C. Wardle,‡ B. E. Argent,* and M. A. Gray*
*Department of Physiological Sciences, University Medical School, Newcastle upon Tyne NE2 4HH, and ‡Paediatric Molecular Genetics, Institute of Molecular Medicine, Oxford University, John Radcliffe Hospital, Oxford OX3 9DU, United Kingdom

ABSTRACT Using the patch clamp technique, we have investigated the blockade of maxi-K^+ channels present on vas deferens epithelial cells by extracellular Ba^{2+}. With symmetrical 140 mM K^+ solutions, Ba^{2+} produced discrete blocking events consisting of both long closings of seconds duration (slow block) and fast closings of milliseconds duration (flickering block). Kinetic analysis showed that flickering block occurred according to an "open channel blocking" scheme and was eliminated by reducing external K^+ to 4.5 mM. Slow block showed a complex voltage-dependence. At potentials between −20 mV and 20 mV, blockade was voltage-dependent; at potentials greater than 20 mV, blockade was voltage-independent, but markedly sensitive to the extracellular K^+ concentration. These data reveal that the vas deferens maxi-K^+ channel has two Ba^{2+} binding sites accessible from the extracellular side. Site one is located at the cytoplasmic side of the gating region and binding to this site causes flickering block. Site two is located close to the extracellular mouth of the channel and binding to this site causes slow block.

INTRODUCTION

Maxi-K^+ channels display an unusual combination of very high conductance and strong selectivity for K^+ over other inorganic cations. A number of structural features of the channel have been proposed to explain these findings, and include negatively charged groups at the mouth of the channel (MacKinnon et al., 1989), multi-ion occupancy (Yellen, 1984a,b; Eisenman et al., 1986; Cecchi et al., 1987), and multiple high affinity K^+ binding sites within the conduction pathway (Neyton and Miller 1988a,b). Ba^{2+} is a potent blocker of maxi-K^+ channels in a number of different cell types (Vergara and Latorre, 1983; Benham et al., 1985; Brown et al., 1988; Sheppard et al., 1988). It has been suggested that Ba^{2+} acts as a transition state analogue for K^+ conduction (Latorre and Miller, 1983), and for this reason has been a very useful probe for investigating ion conduction and occupancy of the channel. A characteristic feature of internal Ba^{2+} block is the appearance of long-lived closing (nonconducting) events of seconds duration, where the blocking rate is much slower than the natural closing rate of the channel. Detailed kinetic analysis of internal Ba^{2+} block suggests that the Ba^{2+} binding site is located some 60–95% of the way through the membrane field (Vergara and Latorre, 1983; Benham et al., 1985; Brown et al., 1988; Sheppard et al., 1988). A simple model was proposed to explain the interaction of Ba^{2+} with the channel, which involved the channel undergoing transitions between three kinetically distinct states; closed, open, and open/blocked (Vergara and Latorre, 1983). In an elegant series of studies, Miller and colleagues (Miller, 1987; Miller et al., 1987) extended this scheme by demonstrating two additional features of Ba^{2+} blockade. First, the kinetics of block are strongly dependent on the gating of the channel, and vary with P_o. Second, there were both open and closed conformations for the blocked channel, which increased the number of kinetic states in the model to four. (Miller, 1987; Miller et al., 1987). Neyton and Miller (1988a,b) then looked at the effect of varying the concentration of K^+, both cytosolic and extracellular, on internal Ba^{2+} block. They showed that an increase in external K^+ from 0 to 10 mM decreased the rate of Ba^{2+} dissociation (lock-in effect), an increase in external K^+ above 100 mM increased the rate of Ba^{2+} dissociation (enhancement effect), and internal K^+ also induced a Ba^{2+} lock-in effect. Overall, this demonstrated that K^+ and Ba^{2+} strongly interact within the conduction pore of the maxi-K^+ channel, and proposed that the conduction pathway of the channel contained four distinct ion binding sites with high affinity for K^+: two sites, internal and external, composed the lock-in sites, a third was the external enhancement site, and the fourth acted as the Ba^{2+} binding site.

In contrast, only a few investigators have looked at block by external Ba^{2+} in detail. Vergara and Latorre (1983) showed that Ba^{2+} produced an identical type of block to that induced by cytoplasmic Ba^{2+}, although the rate of blocking was some 10^3-fold less in maxi-K^+ channels from rat skeletal muscle. The sidedness of Ba^{2+} action was carefully examined by Miller et al. (1987), who concluded that "all of the characteristics of the blocked state are the same from the two sides." Both studies concluded that Ba^{2+} bound to the same site whatever side it was present; the crucial difference was that external Ba^{2+} had a much larger

Received for publication 24 August 1995 and in final form 21 December 1995.

Y. Sohma's present address is Department of Physiology, Osaka Medical College, Takatsuki Osaka 569, Japan.

Address reprint requests to Dr. M. A. Gray, Department of Physiological Sciences, University Medical School, Framlington Place, Newcastle upon Tyne NE2 4HH, UK. Tel.: 44-91-222-7592; Fax: 44-91-222-6706; E-mail: m.a.gray@ncl.ac.uk.

0006-3495/96/03/1316/10 $2.00

energy barrier to overcome to gain access to the blocking site.

The upper (apical) membrane of human vas deferens epithelial cells contains Ca^{2+}-activated, voltage-dependent, maxi-K^+ channels (Sohma et al., 1994). In a preliminary report (Sohma and Gray, 1993), we found that application of 5 mM extracellular Ba^{2+} produced an unexpectedly complicated type of block, with the channel exhibiting discrete blocking events of both seconds duration (slow block) as well as fast closings of milliseconds duration (flickering block). The flickering block has not been described before, and for this reason we decided to investigate in more detail the kinetics of extracellular Ba^{2+} blockade.

MATERIALS AND METHODS

Human vas deferens cell culture

Primary monolayers of vas deferens cells were grown on collagen-coated glass coverslips from explants of second trimester human fetal vas deferens as previously described (Harris and Coleman, 1989). Six normal fetuses obtained within 48 h from midtrimester prostaglandin-induced terminations or spontaneous abortions were used in this study. Once established, two main cell types predominate in the cultures; a large angular cell type that does not appear tightly packed even at confluence, and a relatively small "cobblestone" cell type that always appears in tightly packed colonies. Both cell types have been identified as epithelial cells on the basis of morphological, biochemical, and immunocytochemical evidence (Harris and Coleman, 1989). The cultures were passaged on glass coverslips (passage numbers were between 2 and 8), and 2–4 days later sent from Oxford to Newcastle upon Tyne. After arrival in Newcastle, they were incubated for 1–7 days in the standard growth medium (Harris and Coleman, 1989) minus cholera toxin before electrophysiological studies were performed.

Measurement of single-channel activity

We studied a total of 98 coverslip cultures (between 9 and 28 coverslips from each of the six fetuses). Single-channel recordings were made at 21–23°C using the patch-clamp technique (Hamill et al., 1981). All patches were obtained from the upper surface of small "cobblestone" cells in confluent areas of the monolayers. Full detail of the electrophysiological technique used in this study are described elsewhere (Gray et al., 1990). The tissue bath was grounded, and potential difference across excised, inside-out patches (V_m) was referenced to the extracellular face of the membrane. Junction potentials were measured using a flowing 3 M KCl electrode (Gray et al., 1988), and the appropriate corrections applied to our data.

The Na^+-rich, extracellular-type solution had the following composition (in mM): 138 NaCl, 4.5 KCl, 2 $CaCl_2$, 1 $MgCl_2$, 5 glucose, 10 *N*-2-hydroxyethylpiperazine-*N'*-2-ethanesulfonic acid (HEPES) at pH 7.4. The 25 K^+:115 Na^+ solution contained 115 NaCl, 25 KCl, 2 $CaCl_2$, 1 $MgCl_2$, 5 glucose, 10 HEPES at pH 7.4. The K^+-rich, intracellular-type solution contained 140 KCl, 2 $CaCl_2$, 1 $MgCl_2$, 5 glucose, 10 HEPES at pH 7.4. When these solutions were used in the pipette, the Ca^{2+} concentration in these solutions was fixed at 1 μM using a buffer system containing 2 mM ethyleneglycol-*bis*-(β-aminoethyl ether)-*N,N'*-tetraacetic acid. Glucose was omitted, and they were filtered through a 0.2 μM membrane filter. The free-Ca^{2+}, Mg^{2+}, and Ba^{2+} concentrations in the pipette solutions were calculated using the EQCAL software (Biosoft, Cambridge, UK). In the presence of the maximum Ba^{2+} concentration used (10 mM) the free Ca^{2+} concentration increased to 62 μM. This increase in external Ca^{2+} has no effect on channel gating or activity (data not shown). The calculated free Ba^{2+} concentrations used were 9.78 mM (10 mM), 4.82 mM (5 mM), 1.85 mM (2.0 mM), and 0.383 mM (0.5 mM). We have used these actual concentrations for the data analysis. All other chemicals were purchased from commercial sources and were of the highest purity available.

Data analysis

To determine open-state probability (P_o), open time (t_o) and closed time (t_c) constants, current records were digitized at 2–10 kHz using a CED 1401 interface (Cambridge Electric Design, Cambridge, UK) and analyzed using a two-threshold transition algorithm which employed a 50% threshold-crossing parameter to detect events. P_o was calculated as the fraction of total time that channels were open using a minimum of 60 s of data. When multichannel patches were used for these determinations, we assumed that the total number of channels present was equal to the maximum number of simultaneous current transitions. We have previously shown that in multichannel patches, channels open and close independently of one another (Sohma et al., 1994). In our previous paper (Sohma et al., 1994), we reported that the gating of this maxi-K^+ channel was consistent with the channel having at least two open and two closed states. The faster open-closed kinetics has submillisecond durations (t_{o1} = ~0.2 ms, t_{c1} = ~0.2–0.5 ms). The slower open-closed kinetics has milliseconds durations (t_{o2} = ~2–5 ms, t_{c2} = ~1–2 ms). Because the very fast time constants were not affected by the blocker (data not shown), we have simplified our analysis by concentrating on the slower kinetics and ignoring the faster natural kinetics by choosing appropriate binwidths. To minimize the effect of missed events (openings not reaching threshold) on measured rate constants in the presence of Ba^{2+}, kinetic analysis was performed on data filtered at 5 kHz. Under these conditions only data obtained at high Ba^{2+} concentrations (5 mM) and at strong negative potentials (−60 mV) were found to be subject to any substantial error. In these cases blocked times were overestimated, but this had little quantitative effect on the overall interpretation of results.

We were not able to consistently prepare outside-out patches; therefore, application of Ba^{2+} to the extracellular side of channels was performed by including Ba^{2+} in the pipette solution and making measurements from excised, inside-out patches. To obtain control measurements (i.e., without Ba^{2+}) for each experimental condition, we analyzed at least eight separate patches. This method is valid, because under control conditions in which the concentration of intracellular Ca is 2 mM, maxi-K^+ channels are almost fully open over a wide potential range (Sohma et al., 1994), and P_o is ~0.9. Therefore, errors due to this indirect determination of control values are minimal.

Significance of difference between means was determined using Student's *t*-test. The level of significance was set at $p \leq 0.05$. All values are expressed as mean ± SEM (number of observations).

RESULTS

Fig. 1 *A* shows the effect of internally and externally applied Ba^{2+} on single-channel currents recorded from inside-out patches, excised from the apical membrane of human fetal vas deferens cells. The patches were bathed in symmetrical K^+-rich (140 K) solutions, containing 2 mM Ca^{2+} in the bath. In the absence of Ba^{2+}, the maxi-K^+ channels usually showed only brief closing events of around ms duration (Fig. 1 *Aa*) and P_o remained >0.9 at membrane potentials (V_m) between −40 mV and +60 mV (Fig. 1 *B*, *open circles*).

Exposing the same patch to 5 mM cytoplasmic Ba^{2+} markedly changed gating and introduced very long closed periods of seconds duration (Fig. 1 *Ac*). In addition, as shown in Fig. 1 (*Ac* and *B*) block was voltage-dependent, and increased as the membrane was depolarized, as has been

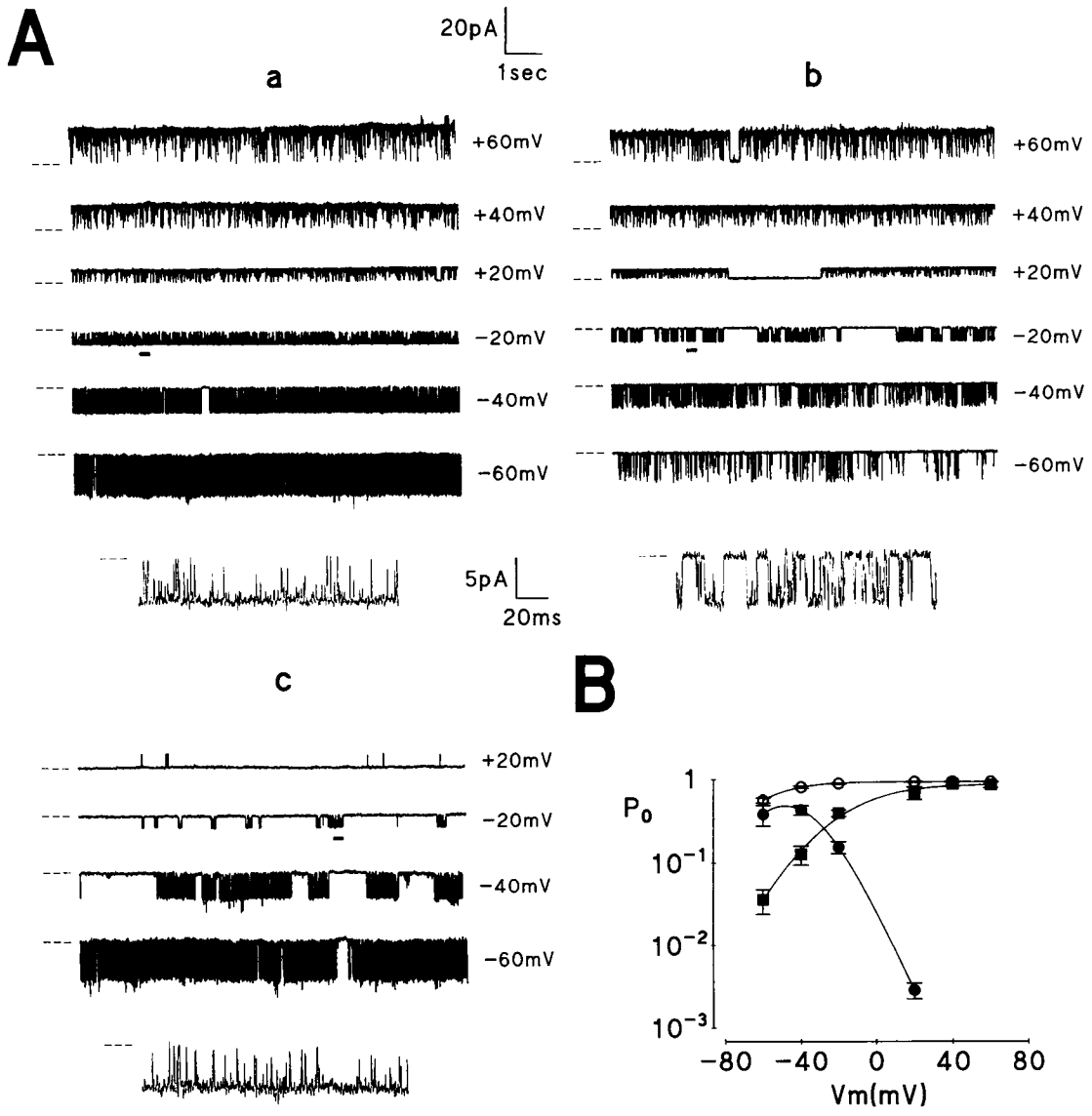

FIGURE 1 Effect of Ba^{2+} on maxi-K^+ channel activity in excised, inside-out patches. (*A*) Typical single-channel currents obtained from patches bathed with symmetrical K^+-rich solutions (140:140), at the membrane potentials (V_m) indicated to the right of each set of traces. The lower expanded traces in *a*, *b*, and *c* show the data marked by the solid lines (at $V_m = -20$ mV) on a faster time base. Dashed lines indicate the closed state of the channel. Data (*a*) under control conditions, (*b*) in the presence of 5 mM extracellular Ba^{2+}, and (*c*) in the presence of 5 mM intracellular Ba^{2+}, low-pass filtered at 1 kHz. (*B*) Semilog plots of open-state probability (P_o) against V_m. Ba^{2+} concentrations: (○) control, (●) 5.0 mM cytoplasmic Ba^{2+}, (■) 5.0 mM extracellular Ba^{2+}. The lines were fit by third-order polynomial least squares regression analysis.

observed in other cells (Vergara and Latorre, 1983; Benham et al., 1985; Miller et al., 1987; Brown et al., 1988; Sheppard et al., 1988). From these data we calculated the zero-voltage dissociation constant ($K_D(0)$) to be $1.1 \times 10^{-4} \pm 1.5 \times 10^{-5}$ M, with $z\delta = 2.5 \pm 0.1$ ($n = 5$) using a method of analysis identical to that of Benham et al. (1985).

Application of 5 mM Ba^{2+} to the extracellular face of the membrane (in a separate patch) also decreased P_o in a voltage-dependent manner, although the polarity was opposite to that observed for intracellular Ba^{2+} (Fig. 1 *B*), and the amount of block was ~25-fold less than for internal Ba^{2+} block. However, close inspection of the current traces in Fig. 1 *Ab* and *c*, shows that the block by external Ba^{2+} was more complex than that observed with cytoplasmic Ba^{2+}. In the presence of extracellular Ba^{2+}, the channel displayed both long closed periods of seconds duration (slow block), similar to that seen with cytoplasmic Ba^{2+} block, and shorter closing events of milliseconds duration (flickering block). This flickering block was not observed in the control condition or in the presence of internal Ba^{2+} (see the expanded traces in *a*, *b* and *c*). These two kinetically distinct closing events occurred simultaneously at $V_m = -20$ mV, but as the membrane was hyperpolarized to potentials greater than −40 mV, the long closed periods seemed to disappear and the flickering closing events became more predominant. In contrast, the channel displayed

only the long closed periods at V_m = 20 mV, and, as the membrane was further depolarized block was relieved. These data reveal that the long closed periods were not caused by Ba^{2+} leaking to the cytoplasmic side because cytoplasmic Ba^{2+} inhibits the channel more strongly at positive V_ms (Fig. 1 *B*). Note that single-channel conductance was not significantly affected by extracellular Ba^{2+} (data not shown).

We next investigated the effect of intracellular and extracellular K^+ concentration on external Ba^{2+} block. For these experiments we chose three external Ba^{2+} concentrations (0.5 mM, 2.0 mM, and 5.0 mM), and compared block using two or three different intracellular K^+ concentrations (140, 25, and 4.5 mM), with extracellular K^+ kept constant at 140 mM. Fig. 2 *Aa* shows typical single-channel currents recorded from an inside-out patch bathed with a K^+-rich solution (140 K) in the pipette and Na^+-rich solution (4.5 K) in the bath. These data show that altering intracellular K^+ has no effect on channel gating (compare with Fig. 1 *Aa*), or on P_o (Fig. 2 *B*), and serves as a control. Fig. 2 *Ab* shows the effect of 5 mM external Ba^{2+} with a 140–4.5 K^+ gradient. In the presence of Ba^{2+} the channel displayed both long-lived closed periods and the flickering closing events of milliseconds duration, which were seen with symmetrical K^+ solutions. However, both kinetic states occurred simultaneously over a wider range of potentials, between −20 and +20 mV, which was not seen with symmetrical K^+ gradients (compare Figs. 1 *Ab* and 2 *Ab*). At potentials <−40 mV, the long closed periods were absent and only the flickering closing events were seen.

In addition to the differences in the pattern of gating, the effect of reducing intracellular K^+ was to increase the amount of block by extracellular Ba^{2+}. This information is summarized in Fig. 2, *C–E*. Overall, a decrease in the bath K^+ from 140 mM to 4.5 mM shifts the relationship between membrane voltage and the degree of Ba^{2+} block toward more depolarized potentials (Fig. 2, *C–E*). Fig. 2, *C–E* also shows that extracellular Ba^{2+} block was dependent on Ba^{2+} concentration.

Kinetics of the "flickering" blockade

We were able to analyze the kinetics of the flickering block in the absence of slow block by holding patches at potentials <−20 mV. Fig. 3, *A* and *B*, shows open- and closed-time histograms for a control channel and for channels exposed to 0.5 and 5.0 mM extracellular Ba^{2+}. Without Ba^{2+}, open- and closed-time histograms showed a single exponential distribution (t_o = 4.98 ± 0.82 ms, t_c = 1.58 ± 0.45 ms, n = 9). However, with both 0.5 and 5.0 mM external Ba^{2+}, a new, slower distribution (t_{cm}) appeared on the closed-time histogram (Fig. 3 *B*), which was independent of Ba^{2+} concentration (t_{cm} 0.5 mM = 18.7 ± 0.6 ms, n = 6; t_{cm} 5.0 mM = 20.9 ± 1.2 ms, n = 6, p = 0.136). Although t_{cm} was independent of blocker concentration, we did find that the frequency of the blocking events was dependent on Ba^{2+} concentration. To compare the frequency of Ba^{2+} blocking events (i.e., the amplitudes from the slower exponential distribution) at different Ba^{2+} concentrations, we calculated the fractional ratio amplitude (FRA). Here the ratio of the Ba^{2+} blocking events to the natural closing events were compared for each experiment and the FRA calculated as follows.

$$\mathrm{FRA} = (A_{cm} \cdot t_{cm})/(A_{cf} \cdot t_{cf}) \quad (1)$$

where A_{cf} and t_{cf}, and A_{cm} and t_{cm} are the y axis intercept (amplitude) and time constant of the faster (natural) and slower (Ba^{2+}-induced) closed-time distributions, respectively. For 0.5 mM Ba^{2+}, FRA was 0.28 ± 0.02 (n = 6) and for 5 mM Ba^{2+} FRA was 0.43 ± 0.04 (n = 6, p = 0.01). Note that t_c in the presence of Ba^{2+} (t_{cf}) was not significantly different from t_c (t_{cf} 0.5 mM = 1.25 ± 0.12 ms, n = 6; t_{cf} 5.0 mM = 1.53 ± 0.10 ms, n = 6). In addition to the effects on the closed-time distribution, external Ba^{2+} also changed the open-time distribution, and t_o in the presence of Ba^{2+} was significantly smaller than the control t_o value (t_o 0.5 mM = 0.62 ± 0.04 ms, n = 6; t_o 5.0 mM = 0.133 ± 0.005 ms, n = 6). Fig. 3 *C* shows that the appearance of t_{cm} in the presence of Ba^+ was not observed for control channels even at low P_o values. This result excludes the possibility that the flickering block is simply due to a shift in the voltage-gating curve of the channel toward more hyperpolarized potentials caused, e.g., by an electrostatic effect of Ba^{2+}. These data implied that Ba^{2+} could interact with the flickering binding site only when the channel opens, according to the following reaction sequence:

$$\underset{\text{Closed}}{C} \underset{\alpha_f}{\overset{\beta_f}{\leftrightarrow}} \underset{\text{Open}}{O} + Ba^{2+} \underset{k_{f-1}}{\overset{k_{f1}[Ba^{2+}]}{\leftrightarrow}} \underset{\text{Open Blocked}}{OBa^{2+}}$$

Scheme 1

In the absence of Ba^{2+} the mean open time is related, at a given potential, to the backward rate constant, α_f, by $t_o = \alpha_f^{-1}$. While in the presence of Ba^{2+}, the mean open time (t_{oBa}) is described by α_f and the flickering blocking rate constant, k_{f1}, as follows:

$$t_{oBa} = 1/(\alpha_f + k_{f1} \cdot [Ba^{2+}]) \quad (2)$$

Because t_{cm} was absent without Ba^{2+} (Fig. 3 *B*), t_{cm} is described by the flickering unblocking rate constant, k_{f-1}, where $t_{cm} = 1/k_{f-1}$.

Therefore,

$$1/t_{oBa} = \alpha_f + k_{f1} \cdot [Ba^{2+}] \quad (3)$$

$$1/t_{cm} = k_{f-1}. \quad (4)$$

Fig. 4 *A* shows a plot of $1/t_{oBa}$ against $[Ba^{2+}]$ for different holding potentials. The data at each potential are well fit by a first-order regression, with the slope of the line and the intercept at the y axis equal to k_{f1} and α_f, respectively. Fig. 4 *B* shows a plot of $1/t_{cm}$ against $[Ba^{2+}]$ at each potential. Between 0 and −40 mV, $1/t_{cm}$ is independent of $[Ba^{2+}]$ and

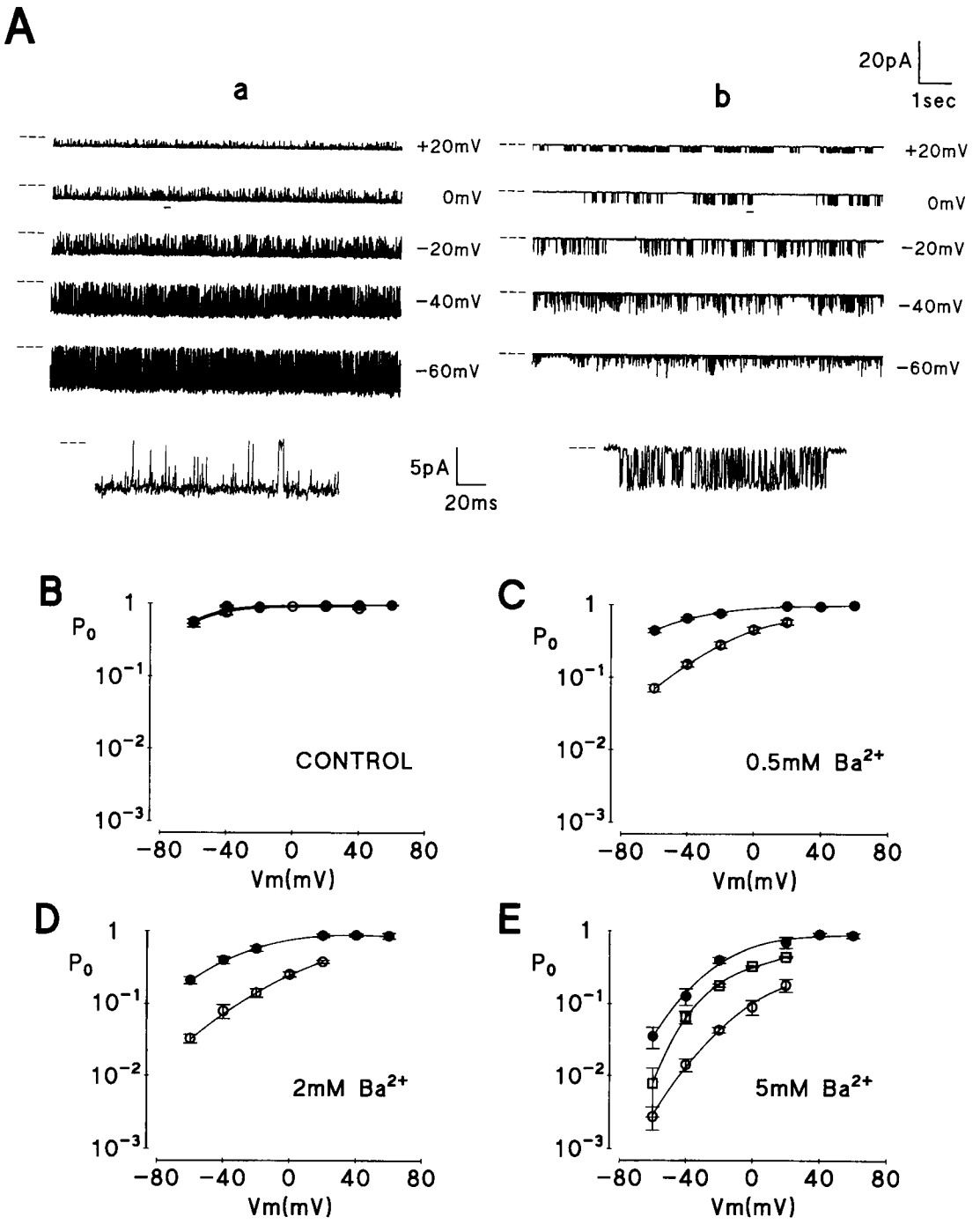

FIGURE 2 Effect of reducing intracellular K^+ on extracellular Ba^{2+} block. (*A*) Typical single-channel currents obtained from patches bathed with asymmetrical K^+-rich solutions, at the membrane potentials (V_m) indicated to the right of each set of traces. The lower expanded traces in *a* and *b* show the data marked by the solid lines (at V_m = 0 mV) on a faster time base. Dashed lines indicate the closed state of the channel. Data (*a*) under control conditions, and (*b*) in the presence of 5 mM extracellular Ba^{2+}. Solutions: pipette, K^+-rich; bath, Na^+-rich (140:4.5). Low-pass filtered at 1 kHz. (*B–E*) Summary of effects of reducing intracellular K^+ on P_o for a range of external Ba^{2+} concentrations. Ba^{2+} concentrations: (*B*) control (n = 8) (*C*) 0.5 mM (n = 5), (*D*) 2.0 mM (n = 5), (*E*) 5.0 mM (n = 5). K^+ concentrations in mM (pipette:bath): (●) 140:140, (□) 140:25, (○) 140:4.5.

equal to k_{f-1}. The $1/t_{cm}$ data at −60 mV shows an apparent $[Ba^{2+}]$-dependence. However, the values with high $[Ba^{2+}]$ could be underestimated because opening events were too brief to record them accurately under these conditions (see Materials and Methods). Nonetheless, the data show that only the on-rate constant is concentration-dependent, a finding that supports the reaction sequence described in Scheme 1.

Using the data obtained from Fig. 4 we then investigated the voltage-dependence of k_{f1} and k_{f-1}. Fig. 5 shows that semilog plots of k_{f1} and k_{f-1} against V_m are well fitted by a

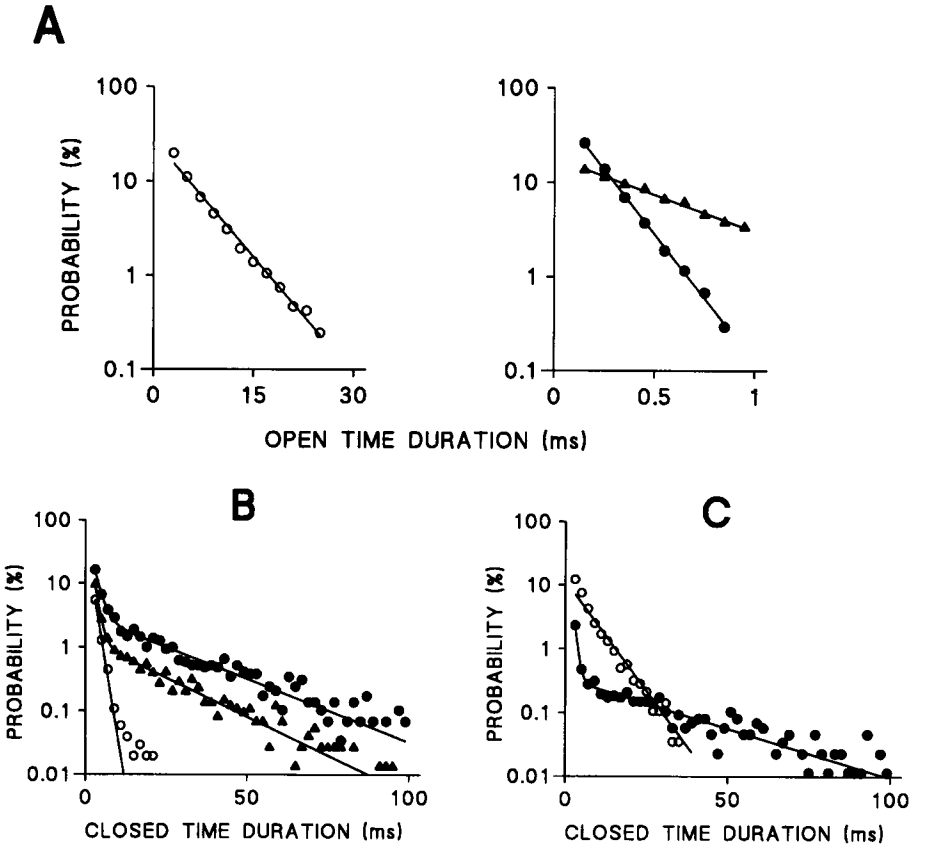

FIGURE 3 Effect of flickering Ba^{2+} block on single-channel kinetics. Semilog plots of (*A*) open-time and (*B* and *C*) closed-time histograms for control (○) and in the presence of extracellular Ba^{2+} (●, ▲). (*A*) Open-time distributions. These were fitted by a single exponential with t_o = 5.3 ms (○), 0.56 ms (▲, 0.5 mM Ba^{2+}) and 0.16 ms (●, 5 mM Ba^{2+}), respectively. Binwidthes are 2 ms (○) and 0.1 ms (●, ▲), respectively. (*B*) Corresponding closed-time distributions. These were fitted by a single exponential (○) with t_c = 1.4 ms, and sum of two exponentials with t_{cf} = 1.3 ms and t_{cm} = 17.9 ms (▲, 0.5 mM Ba^{2+}), and t_{cf} = 1.8 ms and t_{cm} = 21.9 ms (●, 5.0 mM Ba^{2+}), respectively. Values of A_{cf} and A_{cm} were 90.5 and 1.3 (▲), and 74.6 and 3.1 (●), respectively. Binwidth is 2 ms. The current recordings with and without Ba^{2+} used for the analysis were obtained from three different inside-out patches at V_m = −40 mV. (*C*) Effect of P_o on closed-time distributions. For the control data (○) V_m was −90 mV and P_o = 0.30. (●) Data in the presence of 0.5 mM Ba^{2+} at V_m = −20 mV, P_o = 0.31, and for the control channel t_c = 6.33 ms and in the presence of Ba^{2+} t_{cf} = 0.85 ms and t_{cm} = 27.9 ms, respectively. Data filtered at 5 kHz and digitized at 10 kHz. Similar results were found in two other experiments. Solutions: pipette, K^+-rich; bath, Na^+-rich.

first-order regression. Note that the k_{f1} data are well described by a first-order regression even at V_m = 0 mV, a potential at which the slow blockade occurred most frequently. This suggests the influence of the slow blockade on t_{oBa} is negligible. From the best fit to the experimental points the following relationships were obtained:

$$k_{f1} = 10^{5.54} \cdot \exp(-0.0315 \cdot V_m) \quad (M^{-1} \cdot s^{-1}) \quad (5)$$

$$k_{f-1} = 10^{1.28} \cdot \exp(-0.0238 \cdot V_m) \quad (s^{-1}). \quad (6)$$

The k_{f1} and k_{f-1} have an *e*-fold change for 31.7 and 42.0 mV, respectively. Applying Eq. 7 to Eqs. 5 and 6, the values of $z\delta$ in k_{f1} and k_{f-1} are 0.80 and 0.60, respectively.

$$k_{f1,-1} = k_{f1,-1}(0) \cdot \exp(-z\delta FV_m/RT) \quad (7)$$

where F, R, and T have the usual meanings, $k_{f1}(0)$ and $k_{f-1}(0)$ are the zero-voltage "flickering" blocking and unblocking rate constants, respectively, z is the effective charge, and δ is a fraction of membrane potential experienced by the blocking ion (Woodhull, 1973).

The unblocking rate constant, k_{f-1}, showed a similar voltage-dependence, and was of the same polarity, to the blocking rate constant, k_{f1}. The fact that both k_{f1} and k_{f-1} increase with hyperpolarization suggests that Ba^{2+} associates with the flickering binding site from the extracellular side and mainly dissociates from this site, to the cytoplasmic side of the channel. A similar conclusion was reached by Neyton and Miller (1988a,b), when using a high external K^+ concentration.

If we now look at the effect of increasing internal K^+ on external Ba^{2+} block, we find that increasing the cytoplasmic K^+ concentration from 4.5 mM to 140 mM increased k_{f-1} (to $k_{f-1}(0) = 10^{2.84}$ s^{-1}) and importantly changed the polarity of voltage-dependence ($z\delta$ = −0.69) (Fig. 5). These data suggest that changing the gradient of K^+ increases the exit rate of the blocking ion from the channel.

Kinetics of the "slow" Ba^{2+} blockade

We found that the flickering block could be eliminated by keeping the intracellular K^+ concentration at 140 mM and reducing the extracellular K^+. Fig. 6 *A* shows typical single-channel currents obtained from inside-out patches with and without extracellular Ba^{2+}, bathed with the 25 K^+:115 Na^+ solution in the pipette and the 140 K^+-rich solution in the bath (i.e., 25:140). Without Ba^{2+}, the intrinsic properties of the channel were not affected by the reduced external K^+ concentration (Fig. 6 *Aa*). In the presence of 2 mM extracellular Ba^{2+}, channel gating was changed and long-lived nonconducting events were induced. This slow blockade was essentially identical to that observed at positive V_m values with either symmetrical 140 K^+-rich solutions (Fig. 1 *Ab*), or with low intracellular K^+ concentrations (Fig. 2 *Ab*). However, in contrast to these experiments (Figs. 1 and 2), there was no evidence for

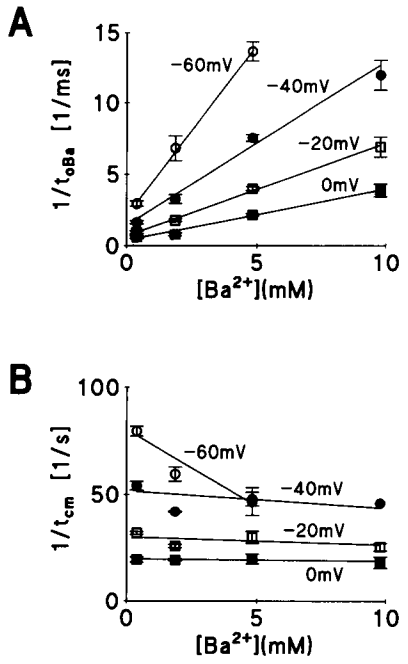

FIGURE 4 Summary of the effect of extracellular $[Ba^{2+}]$ on $1/t_{oBa}$ and $1/t_{cm}$ at different membrane potentials. (*A*) $1/t_{oBa}$ and (B) $1/t_{cm}$. Data are the means of three to six patches at each Ba^{2+} concentration. Solutions: pipette, K^+-rich; bath, Na^+-rich (140:4.5). The lines were fitted by first-order least squares regression analysis.

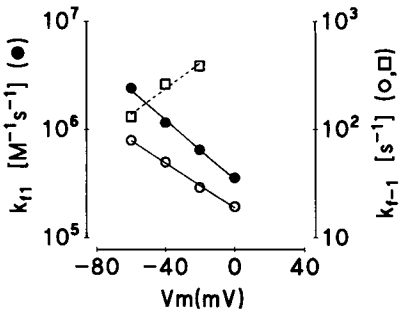

FIGURE 5 Voltage-dependence of k_{f1} and k_{f-1}. The values of k_{f1} and k_{f-1} were calculated from data shown in Fig. 4, *A* and *B*, using Eqs. 3 and 4, respectively. The value of $1/t_{cm}$ at −60 mV is represented by the value at the lowest $[Ba^{2+}]$ in Fig. 4 *B*. k_{f-1} data bathed with symmetrical K^+-rich solutions (□) are superimposed. Data were obtained from six patches containing one active channel and calculated using Eq. 4. The lines were fitted by first-order least squares regression analysis. The fitted parameters are shown in the text. Solutions: pipette, K^+-rich, bath Na^+-rich (140:4.5), apart from (□), which uses symmetrical K^+ solutions (140:140).

the flickering blockade at all V_m values tested (compare Fig. 6 *Ab* with Fig. 1 *Ab* and 2 *Ab*), suggesting that K^+ entering the channel pore from the cytoplasmic side prevents extracellular Ba^{2+} from gaining access to the flickering site, but does not prevent binding to the slow site. Fig. 6 *B* shows the voltage and K^+ concentration-dependence of the slow blockade. When bathed with the 25 K^+:115 Na^+ pipette solution and the 140 K^+-rich bath solution, 2 mM extracellular Ba^{2+} blocked the channel, voltage-independently at potentials >20 mV, but voltage-dependently at potentials <20 mV. Increasing the extracellular K^+ concentration, $[K^+]_{ex}$, from 25 mM to 140 mM decreased the slow block such that the channels were almost fully open at positive V_m values. Note that under these symmetrical conditions, as was shown in Fig. 1, the flickering block was present at potentials <−20 mV. Decreasing $[K^+]_{ex}$ from 25 to 4.5 mM increased the amount of slow block.

One striking feature is that the voltage-dependence of the slow block at negative V_m values was lost at positive V_m values. Note that at potentials <−20 mV, current amplitude was small and P_o low, which made it difficult to obtain sufficient data for determining P_o correctly. Because of the unusual voltage-dependence, our data suggested to us that the slow Ba^{2+} binding site might be situated close to the extracellular mouth of the channel pore. To provide some more evidence for this we looked at the effect of extracellular K^+ concentration on the amount of slow block. Fig. 6 *C* shows the quantitative relationship between extracellular K^+ concentration and the slow block at positive V_m values. The P_o data were well fit by Eq. 8 with an apparent dissociation constant K_{DK} = 19.6 mM.

$$1 - P_o\text{block}/P_o\text{control} = (1 + [K^+]/K_{DK})^{-1} \quad (8)$$

This result indicates that extracellular K^+ behaves as a competitive inhibitor of the slow Ba^{2+} blocking site, even though the flow of K^+ is from the cytoplasmic to the extracellular side, under these conditions. This supports the idea that the slow Ba^{2+} binding site is situated close to the extracellular mouth of the channel pore. It proved technically difficult to obtain sufficiently long records from single channel patches to study the kinetics of the slow block in detail. However, assuming that Ba^{2+} can bind to a single slow binding site independently of the open and closed state of the channel, and that Ba^{2+} binding does not change the normal gating of the channel, the kinetics of the slow blockade can be studied from P_o data using the following relationship:

$$K_{ds} = \frac{[Ba^{2+}] \cdot P_o\text{block}}{P_o\text{control} - P_o\text{block}} \quad (9)$$

where K_{ds} is an "apparent" dissociation constant of the slow blockade.

Fig. 7 illustrates the voltage-dependence of K_{ds} calculated using Eq. 9 from P_o data shown in Fig. 6 *A*. K_{ds} increased voltage-dependently from V_m = −20 to 20 mV with an *e*-fold change for ~11 mV ($z\delta$ = 2.3). At potentials >20 mV, K_{ds} was voltage-independent with a value of 2.4 mM. Although the mechanism of this blockade is still unknown, this feature is not consistent with a simple single-ion channel pore model.

DISCUSSION

Maxi-K^+ channels have been identified on a variety of different cell types (see McManus, 1991, for a recent review), and a feature common to all is their blockade by Ba^{2+} (Vergara and

Latorre, 1983; Benham et al., 1985; Miller et al., 1987; Brown et al., 1988; Sheppard et al., 1988; Gray et al., 1990). In all studies, application of cytoplasmic Ba^{2+} produced discrete, long-lived closing events of seconds duration, where channel block occurs by the binding of a single Ba^{2+} ion to an open channel (Vergara and Latorre, 1983). The reported $K_D(0)$ values when bathed with symmetrical high K^+ ($\geq$100 mM) solutions are between 10^{-4} and 10^{-5}M, very similar to the values we have reported in this paper.

In contrast to the information on intracellular Ba^{2+} block, only a few studies have investigated the effect of extracellular Ba^{2+} in detail. Vergara and Latorre (1983) and Miller et al. (1987) reported that the properties of extracellular Ba^{2+} block of maxi-K^+ channels from rat skeletal muscle was identical to that induced by cytoplasmic Ba^{2+}, although it required a 10,000-fold higher concentration to achieve the same degree of block. However, both studies concluded that Ba^{2+} bound to the same site whatever side it was present, the only difference was that external Ba^{2+} had a much larger energy barrier to overcome to gain access to the blocking site. In other words, Ba^{2+} was viewed as binding to a single, well defined site within the conduction pathway. In addition, this work also suggested that Ba^{2+} entering the channel from either side left the channel by exiting to the internal side, thereby avoiding the larger, extracellular-facing energy barrier.

Evidence for two separate Ba^{2+} binding sites on the vas deferens maxi-K^+ channel

The important aspect of the work presented in this paper is the demonstration of a novel, flickering form of extracellular Ba^{2+} block, in addition to the well documented slow form of block.

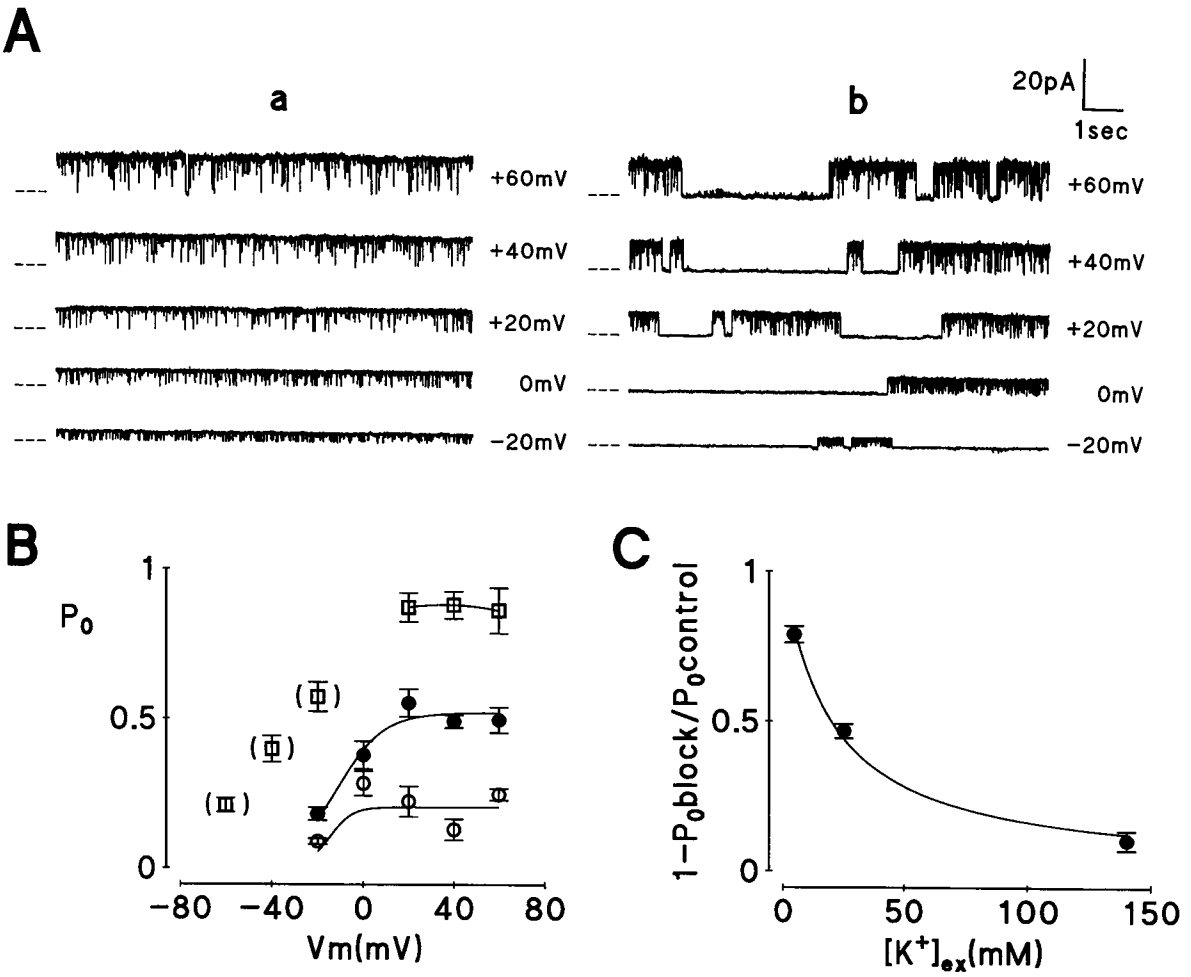

FIGURE 6 Effect of voltage and extracellular K^+ concentration on the slow blockade induced by extracellular Ba^{2+}. (*A*) Typical single-channel currents obtained from patches bathed with asymmetrical K^+-rich solutions, at the membrane potentials (V_m) indicated to the right of each trace. Data (*a*) under control conditions, (*b*) in the presence of 2 mM extracellular Ba^{2+}. Dashed lines indicate the closed state of the channel. Solutions: pipette, 25 K^+:115 Na^+; bath, K^+-rich. Low-pass filtered at 1 kHz. (*B*) Summary of the effects of changing the extracellular K^+ concentration on slow Ba^{2+} blockade. Plots of P_o against V_m are illustrated for different extracellular K^+ concentration. K^+ concentrations in mM (pipette:bath): (□) 140:140 (n = 5), (●) 25:140 (n = 5), (○) 4.5:140 (n = 4). Ba^{2+} concentration: 2 mM. Note that for data points in parentheses, the flickering blockade was detectable. (*C*) Relationship between slow block and extracellular K^+ concentration. The data points were calculated from the results presented in Fig. 6 *B*. P_o data at V_m = 20, 40, and 60 mV were averaged for each K^+ concentration because there was no significant difference between data sets at any two different potentials. The solid line was fitted by Eq. 8.

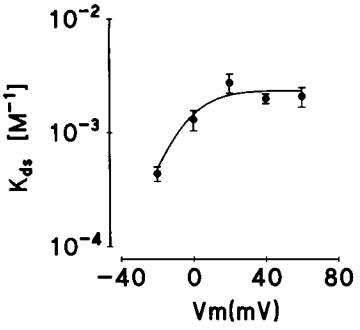

FIGURE 7 Summary of the effect of voltage on the apparent dissociation constant (K_{ds}) for slow Ba^{2+} block. The dissociation constants were obtained from the data in Fig. 6 *B*. K^+ concentrations in mM (pipette:bath): 25:140. The solid line was fitted to the following equation: K_{ds} = max/(1 + exp(a(V_m − V_0))), where max is the maximum K_{ds} value (2.4 mM), a is a slope constant (0.091), and V_0 is the membrane potential at which K_{ds} is half-maximal (−5.1 mV).

The simplest interpretation of this data is that the vas deferens maxi-K^+ channel must have at least two separate Ba^{2+} binding sites to produce the flickering and slow forms of block. Kinetic analysis showed that the flickering Ba^{2+} blockade occurred according to an "open channel blocking" scheme. In support of this, we demonstrated that the flickering association rate constant was voltage- and concentration-dependent, while the dissociation rate constant was independent of blocker concentration. The voltage-dependence of k_{f1} and k_{f-1} bathed with K^+-rich pipette and Na^+-rich bath solutions suggested that Ba^{2+} associated with the flickering binding site from the extracellular side and mainly dissociated from this site to the cytoplasmic side under these conditions. Increasing the cytoplasmic K^+ concentration from 4.5 to 140 mM (with a constant external K^+ of 140 mM) increased k_{f-1} and changed the polarity of of k_{f-1} from a positive to a negative value. This result strongly suggests that K^+ entering the channel from the cytoplasmic side "knocks off" Ba^{2+} bound to the flickering site, increasing its exit rate to the extracellular side of the channel. This "knock-off" effect, first reported by Armstrong (1975), was also observed for Cs^+ block of the Ca^{2+}-activated K^+ channel in chromaffin cell membranes by Yellen (1984b). Flickering blockade was also undetectable when we reduced the extracellular K^+ concentration relative to intracellular, again implying that internal K^+ can destabilize the binding of extracellular Ba^{2+} to the flickering binding site. The fact that Ba^{2+} did not alter the channels natural closing events suggests that the "gating region" of the channel is located between the external mouth of the channel and the flickering Ba^{2+} site. This would place the flickering binding site in a region of the pore, which is found on the cytoplasmic side of the gating region (or possibly within the gating region itself).

The slow block showed an unusual voltage-dependence. It was voltage-dependent between 20 mV and −20 mV, but was voltage-independent at potentials >20 mV. This means that the effective valence ($z\delta$) value changed voltage-dependently. At V_m values of >20 mV, the value of $z\delta$ is approximately zero, and no remarkable change in blocking kinetics was observed (Fig. 6 *B*). In contrast, the data at negative potentials, which exhibit a clear dependence on voltage, implies that the slow binding site is located deep inside ($z\delta$ = 2.3) the conductive pore of the channel from the extracellular side. However, maxi-K^+ channels operate by a multi-ion conduction mechanism (Yellen, 1984a,b; Eisenman et al., 1986; Cecchi et al., 1987; Neyton and Miller, 1988a,b), and as such are able to accommodate more than one ion within the pore of the channel. This makes estimating the position of the binding site on the basis of effective valence values problematic. In addition, the slow block displayed a strong dependence on the extracellular [K^+], such that increasing $[K^+]_{ex}$ decreased the slow blockade in a simple, single-site competitive scheme. Taken together, our feeling is that the slow Ba^{2+} binding site is situated very close to the extracellular mouth of the channel pore. Alternatively, we could reconcile our data by including a "second" slow site (the third Ba^{2+} binding site) in the channel pore.

A possible model of vas deferens maxi-K^+ channel

We propose that the vas deferens maxi-K^+ channel has two separate Ba^{2+} binding sites; a flickering binding site that is situated on the cytoplasmic side of the gating region and a slow binding site, tentatively positioned close to the extracellular mouth of channel. This model therefore implies that the slow binding site is located closer to the extracellular solution (containing Ba^{2+}) than is the flickering binding site. This interpretation is supported by the fact that only the slow type of channel block was observed when the direction of K^+ flow was forced to be from the cytoplasmic to extracellular side, and that the flickering blockade was observed when K^+ current flow was in the opposite direction. If this is the case, in any

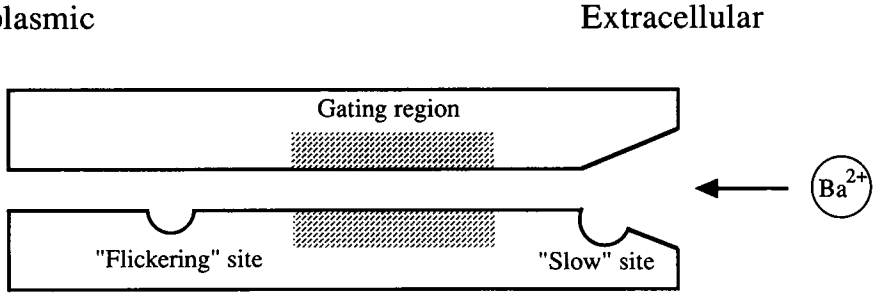

FIGURE 8 A cartoon depicting a possible model of the human vas deferens epithelial maxi-K^+ channel.

single-file channel pore model with two Ba^{2+} binding sites, Ba^{2+} entering from the extracellular side must bind to the slow site before binding to the flickering site. This means that frequency of flickering blockade cannot exceed that of slow blockade. However, it is clear from our data that the flickering blockade occurred much more frequently than the slow blockade. Therefore, it is hard to explain the blocking kinetics by a single-file channel pore model. The simplest solution to this problem is to assume that the slow site is located outside of the single-file region. A possible model that incorporates all of our data is depicted in the cartoon shown in Fig. 8. In this model, it is assumed that Ba^{2+} can bypass the slow site (probably located in the vestibule of the channel), as well as being able to block K^+ entering into the channel pore by binding to the slow site. This model is also consistent with the fact that extracellular K^+ behaved as a competitive inhibitor of the slow Ba^{2+} blockade.

Recently, a putative human maxi-K^+ channel gene (*hSlo*) was cloned from human brain and fetal muscle cDNA libraries (Dworetzky et al., 1994; Pallanck and Ganetzky, 1994), based on sequence similarity to the *mSlo* gene encoding a maxi-K^+ channel cloned from mouse brain and skeletal muscle (Butler et al., 1993), and the *Drosophila* maxi-K^+ slowpoke gene (Adelman et al., 1992). The *hSlo* gene shares 96–98% homology to *mSlo*, and in the putative transmembrane segments S1–S6 and pore region between S5–S6, the amino acid sequence of *hSlo* is completely identical to that of *mSlo*. We can only speculate why the human vas deferens maxi-K^+ channel shows different Ba^{2+}-blocking kinetics from that of the rat or rabbit skeletal muscle maxi-K^+ channel. However, it is possible that segments other than S1–S6 and pore region may affect the blocking kinetics. In this regard the finding by Perez et al. (1994) that the *mSlo* maxi-K^+ is insensitive to charybdotoxin, yet shows very similar Ba^{2+}-blocking kinetics to the skeletal and smooth muscle maxi-K^+ channels, indicates that major pharmacological differences can exist in apparently similar channels. It is also possible that epithelial cells may express different isoforms of the human maxi-K^+ channel compared with excitable tissue, as was recently suggested by the data of Dworetzky et al. (1994).

This work was funded by grants from the Cystic Fibrosis Trust and the Medical Research Council (UK). We thank Mr. David Stephenson for excellent technical assistance.

REFERENCES

Adelman, J. P., K. Z. Shen, M. P. Kavanaugh, R. A. Warren, Y. N. Wu, A. Lagrutta, C. T. Bond, and R. A. North. 1992. Calcium-activated potassium channels expressed from cloned complimentary DNAs. *Neuron.* 9:13–20.

Armstrong, C. M. 1975. Potassium pores of nerve and muscle membrane. *In* Membranes: A Series of Advances, Vol. 3. G. Eisenman, editor. Marcel Dekker, New York. 325–358.

Benham, C. D., T. B. Bolton, R. J. Lang, and T. Takewaki. 1985. The mechanism of action of Ba^{2+} and TEA on single Ca^{2+}-activated K^+-channels in arterial and intestinal smooth muscle cell membranes. *Pfluegers Arch.* 403:120–127.

Brown, P. D., D. D. F. Loo, and E. M. Wright. 1988. Ca^{2+}-activated K^+ channels in the apical membrane of *Necturus* choroid plexus. *J. Membr. Biol.* 105:207–219.

Butler, A., S. Tsunoda, D. P. McCobb, A. Wei, and L. Salkoff. 1993. mSlo, a complex mouse gene encoding "maxi" calcium-activated potassium channels. *Science.* 261:221–224.

Cecchi, X., D. Wolff, O. Alvarez, and R. Lattore. 1987. Mechanisms of Cs^+ blockade in a Ca^{2+}-activated K^+ channel from smooth muscle. *Biophys. J.* 52:707–716.

Dworetzky, S. L., J. T. Trojnacki, and V. K. Gribkoff. 1994. Cloning and expression of a human large-conductance calcium-activated potassium channel. *Mol. Brain Res.* 27:189–193.

Eisenman, G., R. Lattore, and C. Miller. 1986. Multi-ion conduction in the high-conductance Ca^{2+}-activated K^+ channel from skeletal muscle. *Biophys. J.* 50:1025–1034.

Gray, M. A., J. R. Greenwell, and B. E. Argent. 1988. Secretin-regulated chloride channel on the apical plasma membrane of pancreatic duct cells. *J. Membr. Biol.* 105:131–142.

Gray, M. A., J. R. Greenwell, A. J. Garton, and B. E. Argent. 1990. Regulation of maxi-K^+ channels on pancreatic duct cells by cyclic AMP-dependent phosphorylation. *J. Membr. Biol.* 115:203–215.

Hamill, O. P., A. Marty, E. Neher, B. Sakmann, and F. J. Sigworth. 1981. Improved patch-clamp techniques for high-resolution current recording from cells and cell-free membrane patches. *Pfluegers Arch.* 391:85–100.

Harris, A., and L. Coleman. 1989. Ductal epithelial cells cultured from human foetal epididymis and vas deferens: relevance to sterility in cystic fibrosis. *J. Cell Sci.* 92:687–690.

Latorre, R., and C. Miller. 1983. Conduction and selectivity in potassium channels. *J. Membr. Biol.* 71:11–30.

Mackinnon, R., R. Latorre, and C. Miller. 1989. Role of surface electrostatics in the operation of a high-conductance Ca^{2+}-activated K^+ channel. *Biochemistry.* 28:8092–8099.

McManus, O. B. 1991. Calcium-activated potassium channels: regulation by calcium. *J. Bioenerg. Biomembr.* 23:537–560.

Miller, C. 1987. Trapping single ions inside single ion channels. *Biophys. J.* 52:123–126.

Miller, C., R. Latorre, and I. Reisin. 1987. Coupling of voltage-dependent gating and Ba^{2+} block in the high-conductance, Ca^{2+}-activated K^+ channel. *J. Gen. Physiol.* 90:427–449.

Neyton, J., and C. Miller. 1988a. Potassium blocks barium permeation through a calcium-activated potassium channel. *J. Gen. Physiol.* 92:549–567.

Neyton, J., and C. Miller. 1988b. Discrete Ba^{2+} blocks as a probe of ion occupancy and pore structure in the high-conductance Ca^{2+}-activated K^+ channel. *J. Gen. Physiol.* 92:569–586.

Pallanck, L., and B. Ganetzky. 1994. Cloning and characterization of human and mouse homologs of the *Drosophila* calcium-activated potassium channel gene, slowpoke. *Hum. Mol. Genet.* 8:1239–1243.

Perez, G., A. Lagrutta, J. P. Adelman, and T. Toro. 1994. Reconstitution of expressed K_{Ca} channels from *Xenopus* oocytes to lipid bilayers. *Biophys. J.* 66:1022–1027.

Sheppard, D. N., F. Giraldez, and F. V. Sepulveda. 1988. Kinetics of voltage and Ca^{2+} activation and Ba^{2+} blockade of a large-conductance K^+ channel from *Necturus* enterocytes. *J. Membr. Biol.* 105:65–75.

Sohma, Y., and M. A. Gray. 1993. Ba2+ blockade of maxi-K^+ channels on human vas deferens epithelial cells in vitro. *J. Physiol.* 459:423P.

Sohma, Y., A. Harris, C. J. C. Wardle, M. A. Gray, and B. E. Argent. 1994. Maxi-K^+ channels on human vas deferens epithelial cells. *J. Membr. Biol.* 141:69–82.

Vergara, C., and R. Latorre. 1983. Kinetics of Ca^{2+}-activated K^+ channels from rabbit muscle incorporated into planar bilayers. Evidence for a Ca^{2+} and Ba^{2+} blockade. *J. Gen. Physiol.* 82:543–568.

Woodhull, A. M. 1973. Ionic blockage of sodium channels in nerve. *J. Gen. Physiol.* 61:687–708.

Yellen, G. 1984a. Ionic permeation and blockade in Ca^{2+}-activated K^+ channels from bovine chromaffin cells. *J. Gen. Physiol.* 84:157–186.

Yellen, G. 1984b. Relief of Na^+ block of Ca^{2+}-activated K^+ channels by external cations. *J. Gen. Physiol.* 84:187–199.